Raman scattering from vibronic levels of Ni^{3+} in Al_2O_3†

L. L. Chase and C. H. Hao
Physics Department, Indiana University, Bloomington, Indiana 47401
(Received 14 July 1975)

Raman-scattering transitions are observed between low-lying vibronic energy levels of the Jahn-Teller distorted Ni^{3+} ion in Al_2O_3. For an impurity concentration of a few parts per million, the strongest of these transitions has an intensity comparable to that of the strongest vibrational Raman line of the Al_2O_3 host. The lowest singlet level due to hindered rotation of the complex is 60 cm^{-1} above the ground state. A second level is observed at 115 cm^{-1}, and some weaker structure is found in the 250- to 350-cm^{-1} region. The latter may be due in part to impurity-induced scattering from the Al_2O_3 acoustic phonons. The spectra observed in the presence of applied uniaxial strain are fit to calculations based on the cluster model for the vibronic coupling. The parameters deduced from this fit are a rotational constant $\alpha = 43$ cm^{-1} and a rotational barrier height $2\beta = 120$ cm^{-1}. The measured E_g strain coupling coefficient for the ^2E ground state $V_E = 3.6 \times 10^4$ cm^{-1} is used to estimate the stabilization energy $E_{JT} = 1100$ cm^{-1} and the effective cluster vibration frequency $\omega_e = 465$ cm^{-1}. These results are in conflict with the interpretation of earlier acoustic attenuation and dispersion measurements and are in good agreement with more recent models for the vibronic levels deduced from EPR, acoustic resonance, and thermal-conductivity data.

I. INTRODUCTION

In recent years a general and qualitative understanding has been achieved regarding the consequences of the Jahn-Teller (JT) effect for degenerate impurity states in solids.[1-3] However, there has been considerable confusion concerning the interpretation of various types of experimental results in a number of cases. The Ni^{3+} ion substituting at an Al^{3+} site in Al_2O_3 is a notable example, discussed in several recent reviews, in which the original analysis of acoustic attenuation and dispersion measurements[4,5] has recently been shown to be in conflict with electron-spin-resonance,[6,7] thermal-conductivity,[8] and acoustic-paramagnetic-resonance[7] studies. As a consequence, the original interpretation in terms of a strong coupling and an essentially static distortion of the impurity complex is now thought to be incorrect, and the reorientation frequency of the complex is estimated to be ~30 cm^{-1} or larger.[6,7] We present here direct evidence that the vibronic coupling is of intermediate strength, and the lowest reorientation, or tunneling frequency, of the complex is 60 cm^{-1}.

In a previous paper,[9] which will be referred to as GC in the following discussion, we have demonstrated that Raman scattering is a promising new technique for examining the vibronic-energy-level spectrum of orbitally degenerate impurity states in solids. Transitions between the low-lying states resulting from the JT distortion in the vicinity of such an impurity are extremely difficult to observe by direct optical-absorption techniques because they are highly forbidden by selection rules. We find, however, that Raman-scattering transitions between these levels can be observed even at impurity concentrations in the parts-per-million range. The large cross section for these transitions results from the spatial reorientation of the electronic-ground-state orbitals, accompanied by large changes in the optical polarizability, as the distortion of the complex reorients. This reorientation can occur either as a result of the low-frequency quasirotational motions of the distorted complex or it can be produced by the ionic motions resulting from the perturbation of the complex by phonon modes of the host-crystal lattice. The observed spectra, therefore, consist of a number of relatively sharp vibronic levels, at frequencies below the peaks in the phonon density of states, and broader and weaker spectra reflecting the symmetry-projected phonon density of states. Both types of spectra were observed for the Cu^{2+} ion in CaO in GC, and the vibronic transitions were interpreted on the basis of a cluster model for the approximate eigenstates and eigenvalues of the vibronic levels. To simplify this discussion, we adopt the background theory and notation presented in GC with a minimum of discussion.

The Ni^{3+} ion has a $3d^7$ inner-shell configuration. In Al_2O_3, the ground state is derived from the strong-crystal-field (t^6e) configuration, for which a ^2E level lies lowest. The orbital degeneracy of this level is lifted by the degenerate E_g distortions of neighboring oxygen ions, and the orginal electronic degeneracy is replaced by a configurational degeneracy. With the exception of the trigonally-distorted oxygen octahedron at an Al^{3+} site in Al_2O_3, this vibronic coupling problem is identical to that discussed in GC using the cluster model.[10] The trigonal field affects the vibronic levels of the

Ni^{3+} impurity only in second order, and we neglect its influence in the remainder of this discussion.

The parameters involved in the cluster approximation are summarized in the orientational-dependent part of the Schrödinger equation for the vibronic-coupling problem, the derivation of which is outlined in GC,

$$\alpha\frac{\partial^2\Phi}{\partial\phi^2}+(\beta\cos3\phi+\epsilon)\Phi=0\,, \tag{1}$$

where $\Phi(\phi)$ is the angular component, in the configuration space of the E_g coordinates, of the vibronic wave function, α is a rotational splitting parameter, 2β is the energy barrier between equivalent minima for the distorted complex, and ϵ is the energy of the eigenstates referred to the E_g ground state. The parameter ϕ determines the spatial orientation of the distortion through the relation

$$\begin{pmatrix}Q_\theta\\ Q_\epsilon\end{pmatrix}=\rho\begin{pmatrix}\cos\phi\\ \sin\phi\end{pmatrix}, \tag{2}$$

where Q_θ and Q_ϵ are the degenerate E_g-symmetry "cluster distortions" of the complex, and ρ is the modulus of the distortion.

II. EXPERIMENTAL RESULTS

The apparatus used to observe the impurity-induced scattering with applied uniaxial strain has been discussed in GC. The samples used in this work contained about 30 ppm of Ni of which only a fraction, less than 10 ppm, was in the trivalent state. The uniaxial strain experiments were performed on a sample of approximate dimensions $1\times2.5\times4$ mm^3. The strain was applied parallel to the long dimension which was oriented along a diad $\langle11\bar{2}0\rangle$ crystallographic axis. The incident light propagated along the c axis [0001] and the scattered light was collected along a bisectrix $\langle10\bar{1}0\rangle$ axis.

The E_g-symmetry spectra observed at 4.2 and 77°K are shown in Fig. 1. None of the structure observed below 350 cm^{-1} is present in the A_{1g} geometry or in samples of pure Al_2O_3. The intense line at 380 cm^{-1} as a Raman-active E_g-symmetry vibration of Al_2O_3.[11] With the application of uniaxial stress along $\langle11\bar{2}0\rangle$, the 60-cm^{-1} peak shifts upward in frequency, and a very sharp transition appears at low frequency shifts. The low-frequency zero-stress data and a spectrum taken at a stress of 25 kg/mm^2 are presented for comparison in Fig. 2. The low-frequency peak in Fig. 2(b) has a peak intensity comparable with that of the strongest Raman-active optical phonon of Al_2O_3, and its width, observed with higher resolution, is about 1 cm^{-1}. Since a portion of this width may be due

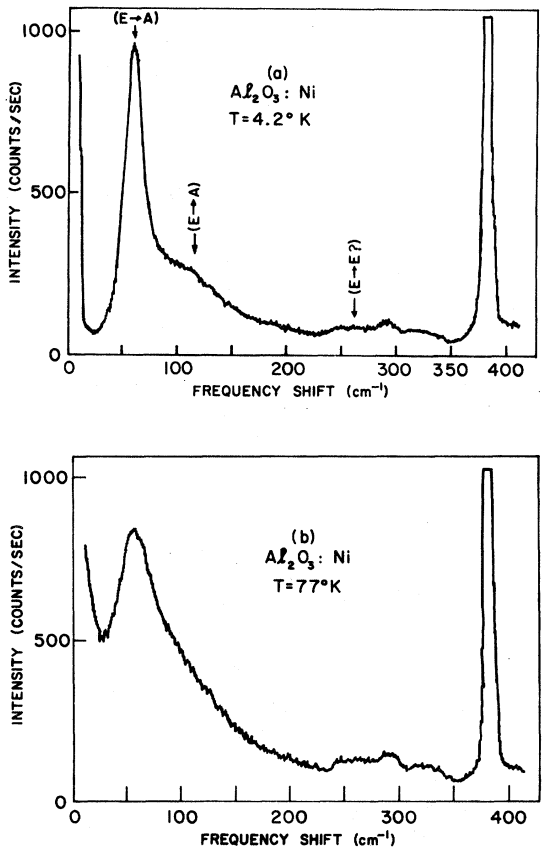

FIG. 1. Raman spectra observed for Ni^{3+} in Al_2O_3 for an E_g-symmetry polarization geometry $X(ZX)Y$. None of the features below 350 cm^{-1} in this spectrum are observable in A_{1g} scattering or in pure Al_2O_3.

to inhomogeneity of the applied strain, this is an estimate of an upper limit on the random strain broadening of the Ni^{3+} ground state in this sample. However, this may not be typical since this sample may be exceptionally free of random strains and other defects, as judged by its extremely low elastic scattering. The strain dependences of the 60-cm^{-1} peak and the ground state splitting are shown in Fig. 3. The strain dependence of the other, broader features in the spectrum could not be determined with meaningful accuracy. However, the broad shoulder at about 115 cm^{-1} and the three broad features between 250 and 350 cm^{-1} moved up in frequency with increasing stress.

III. DISCUSSION

The features to be fit to a vibronic-energy-level scheme in the zero-strain spectrum of Fig. 1 are the relatively sharp peak at 60 cm^{-1}, the shoulder at ~115 cm^{-1}, and the weaker features in the 250–350-cm^{-1} region. If the coupling is assumed to be intermediate in strength so that the 60-cm^{-1} line corresponds to the transition to the first ex-

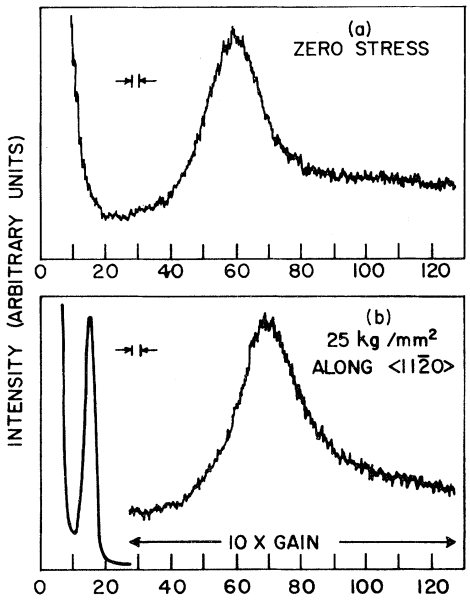

FIG. 2. Uniaxial stress dependence of the low-frequency part of the spectrum of Fig. 1. The width of the 17-cm^{-1} transition between the strain-split sublevels of the E_g ground state is limited by spectrometer resolution. Its true width is about 1 cm^{-1}.

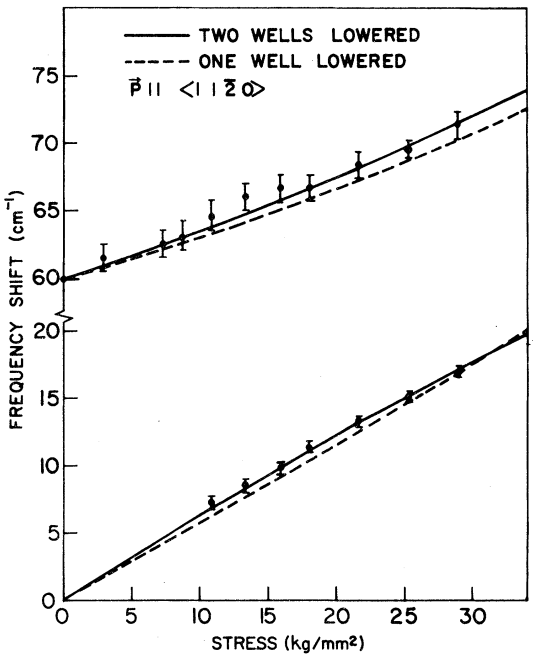

FIG. 3. Uniaxial stress dependence of the low-frequency lines of Fig. 2(b). Solid and dashed curves are fit to the solutions of Eqs. (1) and (3) with $\alpha = 43$ cm^{-1}, $\beta = 60$ cm^{-1}, and $V_E = 3.6\times 10^4$ cm^{-1}. Note the break in the vertical scale above 20 cm^{-1}.

cited hindered rotational state ($E \rightarrow A$), then the parameters $\alpha \simeq 43$ cm^{-1}, $\beta \simeq 60$ cm^{-1} give the transitions, calculated from the cluster model,[9] indicated in Fig. 1. The terminal state of the 115-cm^{-1} transition is assigned to the second A_g level derived from the $j = \frac{3}{2}$ rotational state and the $E(\frac{1}{2}) \rightarrow E(\frac{5}{2})$ transition falls near the lowest frequency peak in the 250–350-cm^{-1} region. It is quite possible that some or all of the structure in this latter region is due to impurity-induced Raman scattering from the zone-boundary acoustic modes of Al_2O_3. Without a detailed knowledge of the phonon density of states, this possibility cannot be explored further.

This interpretation of the observed zero-stress spectrum can be further tested in two ways using the uniaxial stress data. The stress dependence of the quasirotational eigenvalues can be calculated approximately by the methods indicated in GC. The terms which must be added to the Hamiltonian of Eq. (1) are[9]

$$H(\text{strain}) = V_E(e_\theta \cos\phi + e_\epsilon \sin\phi)\,, \tag{3}$$

where V_E is a strain coupling coefficient and e_θ and e_ϵ are the symmetrized strain components referred to the axes of the approximate oxygen octahedron surrounding the impurity. An applied stress P along $\langle 11\bar{2}0\rangle$ is approximately along a $\langle 110\rangle$ direction of this octahedron and produces symmetrized strain components, referred to octahedral symmetry,

$$e_\theta \simeq -(S_{11} - \tfrac{1}{2}S_{12} - \tfrac{1}{2}S_{13})\tfrac{1}{2}P\,,$$
$$e_\epsilon = 0\,, \tag{4}$$

where the trigonal deformation of the octahedron is allowed for to first order by the use of both S_{12} and S_{13}. For a compressive stress, $P<0$ and $e_\theta > 0$. The only additional parameters required to calculate the strain dependence of the quasirotational levels are V_E and the sign of $V_E\beta$. The latter determines whether one or two of the three ϕ-dependent potential minima are lowered in energy by a positive e_θ stress. The magnitude of V_E is chosen to best fit the strain splitting of the E_g ground state. The calculations for the values of α and β given above, are shown as solid curves for two wells lowered and dotted curves for one well lowered in Fig. 3. The curvature of the ground-state splitting (lower curve) is due primarily to the strain-induced coupling of the E_g ground state to the A_g level at 60 cm^{-1} for zero strain. This curvature, as well as the strain dependence of the lowest A_g level are clearly fit best by the calculations for two minima lowered by a compressive stress along $\langle 11\bar{2}0\rangle$. The magnitude of $V_E = 3.6\times 10^4$ cm^{-1} is obtained from the fit to the data of Fig. 3.

We have attempted to fit these data by considerably different values of the ratio β/α, which is 1.4 for the curves of Fig. 3. For $\beta/\alpha<0.8$, the calculations fall noticably below the dotted line for the 60-cm^{-1} level for either sign of $V_E\beta$. The 115-cm^{-1} shoulder would also be unexplained with that choice of parameters. In the opposite limit where $\beta/\alpha \gg 1$, the ground state could be assumed to consist of the nearly degenerate $E_g + A_g$ levels, with a small tunneling splitting. This is the initial interpretation advanced to explain acoustic loss and dispersion[4,5] and early ESR[12] measurements. The 60-cm^{-1} line would then correspond to the transition to the second singlet level derived from $j=\frac{3}{2}$. The calculations for that case cannot be fit to the data since one component of the 60-cm^{-1} transition would remain at constant frequency, and a second transition, $E(\frac{1}{2}) \rightarrow E(\frac{5}{2})$, would be observed moving upward in energy with nearly twice the slope of the data points. The values of α and β given above are, therefore, not only consistent with the existence of the 115-cm^{-1} shoulder, but they are also in the only range of parameters which fits the strain dependence of the levels.

The measured coupling coefficient V_E can be used to relate the measured α to an effective frequency for the "cluster vibration" as discussed in GC. Ham[13] has derived a relation between V_E and the linear JT coupling term V_1 in the vibronic Hamiltonian of the ^2E level[2,13]

$$H = (P_\theta^2 + P_\epsilon^2)/2\mu + \tfrac{1}{2}\mu\omega_e^2(Q_\theta^2 + Q_\epsilon^2) + V_1(U_\theta Q_\theta + U_\epsilon Q_\epsilon)\,, \tag{5}$$

where the Q_j and P_j are the coordinates and momenta of the E_g cluster vibration, μ is the mass of an oxygen ion, ω_e is an effective vibrational frequency, and the U_j are electronic operators in the basis of the ^2E orbitals. The relation is

$$V_1 = \sqrt{3}\,V_E/2R\,, \tag{6}$$

where R is the average Al^{3+}-O^{2-} separation in this case. The adiabatic stabilization energy of the complex is then

$$E_{JT} = V_1^2/2\mu\omega_e^2\,, \tag{7}$$

and this is related to α by

$$\alpha = (\hbar\omega_e)^2/4E_{JT}\,. \tag{8}$$

Combining Eqs. (6)–(8), we obtain an effective mode frequency $\omega_B \simeq 465\ cm^{-1}$ and a stabilization energy $E_{JT} \simeq 1100\ cm^{-1}$. For comparison with this value of ω_e, the average frequency of the seven Raman-active zone-center optic phonons of Al_2O_3 is $520\ cm^{-1}$.[11] Considering that the density-of-states peaks of the three zone-boundary acoustic modes would tend to lower this average, the above value of ω_e for which the strain coefficient is consistent with the experimental value of α is quite reasonable. It is, however, possible that this agreement is merely fortuitous since the measured V_E for Cu^{2+} in[9] CaO was too small by a factor of 2.5 to account for the observed vibronic structure. That disagreement was attributed to the inapplicability of Eq. (6) due mainly to the large coupling to the oxygen polarization and also to the second-nearest neighbors. A summary of the parameters obtained or estimated from the Raman-scattering data is given in Table I.

TABLE I. Cluster-model parameters for Ni^{3+} in Al_2O_3. All energies are in cm^{-1}.

α	β	V_E	E_{JT}	ω_e
43	60	3.6×10^4	1100	465

The observation that a compressive stress along a $\langle 110\rangle$ direction of the oxygen octahedron, corresponding to $e_\theta > 0$, leads to a lowering of two of the three potential minima implies that $V_1\beta < 0$. Since $V_1 > 0$ is most likely for a single e orbital,[3] we conclude that $\beta < 0$ and the minima of the ϕ dependence of the adiabatic potential stabilize a compressed distortion of the octahedron [$\phi = \pm\frac{1}{3}\pi$, π in Eq. (2)].

IV. CONCLUSION

We conclude that the vibronic coupling for Ni^{3+} in Al_2O_3 is of intermediate strength, and the first vibronic excited state is 60 cm^{-1} above the ground doublet. It is likely that this excited singlet is responsible for the resonance at 55 cm^{-1} in thermal-conductivity measurements[8] and for the heat-pulse absorption observed by Hu *et al.*[14] The main factor responsible for the large rotational splittings for Ni^{3+} in Al_2O_3 is the hardness of the host lattice. If, for example, $\omega_e \sim 300\ cm^{-1}$, the use of the measured V_E in Eqs. 6–8 would give $\alpha \sim 8\ cm^{-1}$ and $E_{JT} \sim 2500\ cm^{-1}$, and the lowest excited singlet would be only a few cm^{-1} above the ground state.

The surprisingly large intensity of the vibronic scattering with an impurity concentration of only a few parts per million suggests that Raman scattering will be generally applicable to the study of vibronic coupling in orbitally degenerate states.

ACKNOWLEDGMENTS

We are grateful to Dr. Patrick Hu and Dr. V. Narayanamurti of Bell Telephone Laboratories for the use of their Al_2O_3 sample.

†Research Supported by National Science Foundation Grant No. DMR72-03015.

[1]M. D. Sturge, in *Solid State Physics*, edited by F. Seitz and D. Turnbull, (Academic, New York, 1967), Vol. 20.

[2]F. S. Ham, in *Electron Paramagnetic Resonance*, edited by S. Geschwind (Plenum, New York, 1972).

[3]R. Englman, *The Jahn-Teller Effect in Molecules and Crystals* (Wiley-Interscience, New York, 1972).

[4]E. M. Gyorgy, M. D. Sturge, D. B. Fraser, and R. C. LeCraw, Phys. Rev. Lett. 15, 19 (1965).

[5]M. D. Sturge, J. T. Krause, E. M. Gyorgy, R. C. LeCraw, and F. R. Merritt, Phys. Rev. 155, 218 (1967).

[6]L. N. Shen and T. L. Estle, Bull. Am. Phys. Soc. 17, 263 (1972).

[7]M. Abou Ghantous, C. A. Bates, I. A. Clark, J. R. Fletcher, P. C. Jaussaud, and W. S. Moore, J. Phys. C 7, 2707 (1974).

[8]M. Locatelli and A. M. de Goër, Solid State Commun. 14, 111 (1974).

[9]S. Guha and L. L. Chase, Phys. Rev. Lett. 32, 869 (1974); Phys. Rev. B 12, 1658 (1975).

[10]The conditions necessary for the applicability of the cluster model have been discussed recently by J. R. Fletcher, J. Phys. C 5, 852 (1972), and by M. C. M. Obrien, *ibid.* 5, 2045 (1972).

[11]S. P. S. Porto and R. S. Krishnan, J. Chem. Phys. 47, 1009 (1967).

[12]S. Geschwind and J. P. Remeika, J. Appl. Phys. 33, 370 (1962).

[13]F. S. Ham, Phys. Rev. 166, 307 (1968).

[14]P. Hu, V. Narayanamurti, and R. C. Dynes, Bull. Am. Phys. Soc. 19, 337 (1974).